AFRL-RX-WP-TM-2010-4089

COLLABORATIVE RESEARCH AND DEVELOPMENT CONTRACT

Delivery Order 0052: Microvascular Composites

David M. Phillips

Universal Technology Corporation

MAY 2008
Final Report

AIR FORCE RESEARCH LABORATORY
MATERIALS AND MANUFACTURING DIRECTORATE
WRIGHT-PATTERSON AIR FORCE BASE, OH 45433-7750
AIR FORCE MATERIEL COMMAND
UNITED STATES AIR FORCE

NOTICE AND SIGNATURE PAGE

Using Government drawings, specifications, or other data included in this document for any purpose other than Government procurement does not in any way obligate the U.S. Government. The fact that the Government formulated or supplied the drawings, specifications, or other data does not license the holder or any other person or corporation; or convey any rights or permission to manufacture, use, or sell any patented invention that may relate to them.

This report was cleared for public release by the Wright-Patterson Public Affairs Office and is available to the general public, including foreign nationals. Copies may be obtained from the Defense Technical Information Center (DTIC) (http://www.dtic.mil).

AFRL-RX-WP-TM-2010-4089 HAS BEEN REVIEWED AND IS APPROVED FOR PUBLICATION IN ACCORDANCE WITH ASSIGNED DISTRIBUTION STATEMENT.

*//Signature//	//Signature//
MARK N. GROFF	ROBERT ENGHAUSER

This report is published in the interest of scientific and technical information exchange, and its publication does not constitute the Government's approval or disapproval of its ideas or findings.

*Disseminated copies will show "//Signature//" stamped or typed above the signature blocks.

REPORT DOCUMENTATION PAGE

Form Approved
OMB No. 0704-0188

1. REPORT DATE *(DD-MM-YY)*	2. REPORT TYPE	3. DATES COVERED *(From - To)*
May 2008	Final	03 May 2006 – 01 May 2008

4. TITLE AND SUBTITLE
COLLABORATIVE RESEARCH AND DEVELOPMENT CONTRACT
Delivery Order 0052: Microvascular Composites

5a. CONTRACT NUMBER
F33615-03-D-5801-0052

5b. GRANT NUMBER

5c. PROGRAM ELEMENT NUMBER
62102F

6. AUTHOR(S)
David M. Phillips

5d. PROJECT NUMBER
4349

5e. TASK NUMBER
L0

5f. WORK UNIT NUMBER
4349L0VT

7. PERFORMING ORGANIZATION NAME(S) AND ADDRESS(ES)
Universal Technology Corporation
1270 North Fairfield Road
Dayton, OH 45432-2600

8. PERFORMING ORGANIZATION REPORT NUMBER
S-531-052

9. SPONSORING/MONITORING AGENCY NAME(S) AND ADDRESS(ES)
Air Force Research Laboratory
Materials and Manufacturing Directorate
Wright-Patterson Air Force Base, OH 45433-7750
Air Force Materiel Command
United States Air Force

10. SPONSORING/MONITORING AGENCY ACRONYM(S)
AFRL/RXOB

11. SPONSORING/MONITORING AGENCY REPORT NUMBER(S)
AFRL-RX-WP-TM-2010-4089

12. DISTRIBUTION/AVAILABILITY STATEMENT
Approved for public release; distribution unlimited.

13. SUPPLEMENTARY NOTES
PAO case number 88ABW-2009-0041, cleared 01 February 2009. Report contains color.

14. ABSTRACT
This research in support of the Air Force Research Laboratory Materials and Manufacturing Directorate was conducted from 3 May 2006 through 1 May 2008. This task worked to develop new classes of composite materials with mass transporting and sensing capability for improved performance in structural applications. Structures that have embedded microfluidic networks have the potential to bring a range of multifunctionality and adaptability to aerospace structures including active cooling, self-healing, structural health monitoring, and morphing structures. This will ultimately enable increased persistence, responsiveness, and multi-mission capability of structures that use this technology. We examine fiber-reinforced polymer composite processing techniques to create scalable, hierarchical fluidic networks within polymer-based hybrid materials. This includes the investigation of microvascular composite fabrication methods for lined and unlined channel formation, investigation of fundamental thermal transport characteristics, and characterization of the range of adaptive mechanical properties.

15. SUBJECT TERMS
Microfluidic networks, Fiber-reinforced polymer composite

16. SECURITY CLASSIFICATION OF:			17. LIMITATION OF ABSTRACT:	18. NUMBER OF PAGES	19a. NAME OF RESPONSIBLE PERSON (Monitor)
a. REPORT	b. ABSTRACT	c. THIS PAGE			Mark N. Groff
Unclassified	Unclassified	Unclassified	SAR	20	19b. TELEPHONE NUMBER *(Include Area Code)* N/A

Standard Form 298 (Rev. 8-98)
Prescribed by ANSI Std. Z39-18

Abstract

Structures that have embedded microfluidic networks have the potential to bring a range of multifunctionality and adaptability to aerospace structures including active cooling, self-healing, structural health monitoring, and morphing structures. This will ultimately enable increased persistence, responsiveness, and multi-mission capability of structures that use this technology. We examine fiber-reinforced polymer composite processing techniques to create scalable, hierarchical fluidic networks within polymer-based hybrid materials. This includes the investigation of microvascular composite fabrication methods for lined and unlined channel formation, investigation of fundamental thermal transport characteristics, and characterization of the range of adaptive mechanical properties.

Introduction

Imagine an aircraft skin with an artificial circulatory system that enables autonomic temperature regulation, dynamic mechanical response, transpiration cooling, and self-healing of the vehicle similar to a living organism. Such bio-inspired concepts are driving the development of adaptive composites that mimic this responsive functionality over a broader range of extreme operational environments. Correspondingly, there is a need to understand the fundamental science of fabrication and multifunctional design of these adaptive composites. Traditionally, the high-performance, load-bearing sub-structures of aircraft, satellites and robots have been rigid, passive, and structurally efficient. Active system functionalities such as electronics, sensors, controls, energy storage, or energy harvesting are conventionally added by attaching components to the rigid structure. While this compartmentalization of functions into attached subsystems streamlines assembly and facilitates easy maintenance or upgrades, it also increases part count, slows assembly, adds weight, and decreases the level of integration. This modular approach is in stark contrast to the highly integrated, redundant, hierarchical, self-regulating, and adaptive systems in natural organisms. An example of such a subsystem is the mass-transporting networks within animals and the optimally arranged xylem and phloem vessels of vascular plants.[i] By including fluids and associated mass transport within the composite, a wide range of "life-like" properties can be envisioned. However, the corresponding complexity, balancing of multifunctional properties, and sustainability of using fluidic networks within structures also poses substantial scientific and engineering challenges. This proposed effort seeks to create methods and understanding regarding how mass-transporting networks can be incorporated into structural hybrid composites using scalable, composite-like processing methods to impart numerous multifunctional properties without significantly impacting structural properties. Specifically, the use of microvascular

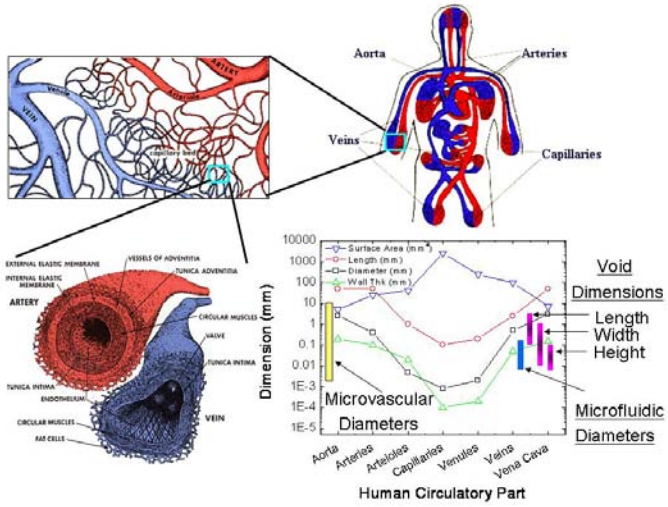

Figure 1. The Human Circulatory System – an Inspiring Hiearchical and Multi-functional Microfluidic System.

composites to actively cool, to transport material for subsequent reconfiguration, and to respond to damage is proposed with the potential for the realization of synergistic, nonlinear coupling between multiple interactions.

Size Consideration

The choice of microvascular passage diameter depends on several factors. The first is mechanical considerations where a large diameter vascular network could adversely affect the mechanical properties of composites. The second is flow rate considerations. Flow rate is governed mainly by the Hagen-Poiseuille relation:

$$\Delta P = 128\mu LQ\cdot(\pi d)^{-4}, \qquad [1]$$

where ΔP is the pressure drop, μ is the dynamic viscosity, L is the passage length, Q is the volumetric flow rate, π is the constant Pi, and d is the passage diameter. These two opposing considerations must be balanced to achieve desired vascular flow rates while maintaining the mechanical robustness of the composite. Biology has tackled many of these issues with the vascular networks present in plants and animals. A multi-scale approach and associated fabrication techniques will be needed to realize the full potential of microvascular systems.

Fabrication Techniques

The desired goal of microvascular processing techniques is integrate it with existing composite processing technology. This would include VARTM (vacuum assisted resin transfer method) and autoclave techniques. Both the composite processing method and the desired vascular passage size affect the choice for microvascular processing. The initial phase of this research focused on the microvascular processing techniques.

Tube Extraction

Tube extraction is applicable to larger vascular passages in a composite, which typically has diameters that span mm to cm. This method involves the use of hollow shrink tubes made from PTFE or FEP, which shrink at 343° C or 190° C, respectively. The tube shrink temperature is chosen so that the tubes shrink after the resin has cured. When the shrinkage occurs, the tube walls pull away from the resin and the low friction surface allows for them to be extracted.

The advantages of this method are that it allows for changing diameters, branched networks, and preformed networks that can be placed into a composite. The disadvantages are join leakage, autoclave incompatibility, and extraction difficulties for tortuous pathways. The networks must also be designed so that all tubes can be reached at the exterior of the cured composite for extraction. This may have some use with VARTM techniques.

High Temperature Wax

High temperature wax was used to mold microvascular passages spannimg diameters from 100μm to 1+cm. The COTS Machinable Wax was purchased from Freeman Mfg. and Supply Co, Avon, OH, where it's intended use if for rapid prototyping and testing of machining operations. The softening point of this wax is relatively low at 108° C. It is chemically compatible with Epoxy based resins.

To manufacture microvascular passages, the wax can be cast and/or machined into preformed networks. Due to the relatively low softening point, this wax is not compatible with autoclave curing techniques. The wax also suffers from a relatively large CTE of $1.71\cdot10^{-5}$

(mm/mm/°C), which can lead to vascular network deformation. The wax is extracted after curing the composite by liquefying the wax and purging with a secondary fluid.

The advantages of the high temperature wax technique are complicated flow networks can be easily manufactured and that networks can be quickly cast from a mold. The disadvantages are numerous besides the previously mentioned low softening point and CTE issues. The most critical issue is the wax extraction due to the amount of wax that can be trapped in the vascular passages.

Another use for high temperature wax is to coat polymer or metal fibers and rods to form a liquid boundary layer for extraction. The technique is still limited by the tortuosity of the vascular passages. This coating technique does not allow for complicated vascular networks like the pure wax.

Soluble Fiber

For the soluble fiber technique, we used a COTS product called Solvron (Nitivy Company Ltd., Tokyo, Japan), which is a water soluble PVA yarn. PVA is commonly used for mold releases for hydrophobic resins, such as epoxies. The size range for the Solvron yarn extends down to a diameter of 60µm for a monofilament. Larger diameters are possible with multifilament yarns or PVA tubes, such as the COTS Povinal tubing (Randolph Austin Company, Manchaca, TX).

Both PVA yarns and tubes were tested for this work with Epoxy based resins. The yarns are compatible with autoclave processing techniques, while the tubes are not. This type of processing is a promising technique for creating unlined microvascular passages for crack detection and self-healing purposes, as the vascular mold material is dissolved by boiling water and removed. Some of the issues encountered with the extraction process are slow rates. This is fueled by both the aspect ratios of the passages and the molecular weight of the PVA, which must be high for fibers to be extruded. The high molecular weight yields a viscous solution, which ultimately must diffuse out of a high aspect ratio passage.

Some advantages of this technique are the capability to solution cast vascular networks, solvent weld various pieces together for branched networks, and the potential to use 3D rapid prototyping print techniques. Exploring a lower molecular weight PVA would also be highly advantageous for template dissolution and removal. This technique warrants further investigation.

Fiber Extraction

Fiber extraction techniques focus on the smaller diameters. We utilized COTS fluorinated (FEP) fishing line for this purpose. Seaguar (New York, NY) Grand Max FX tippet in diameters 90µm, 128µm, and 205µm had tensile strengths of 41N, 80N, and 198N, respectively. These fibers were cured in neat Epon 862 with Cure W resin and the extraction force was recorded. As seen in Fig. 2, the possible pullout lengths for these fibers are 3.1m, 3.9m, and 6.9m for the 90µm, 128µm, and 205µm diameters, respectively from the Epon 862/W cured resin.

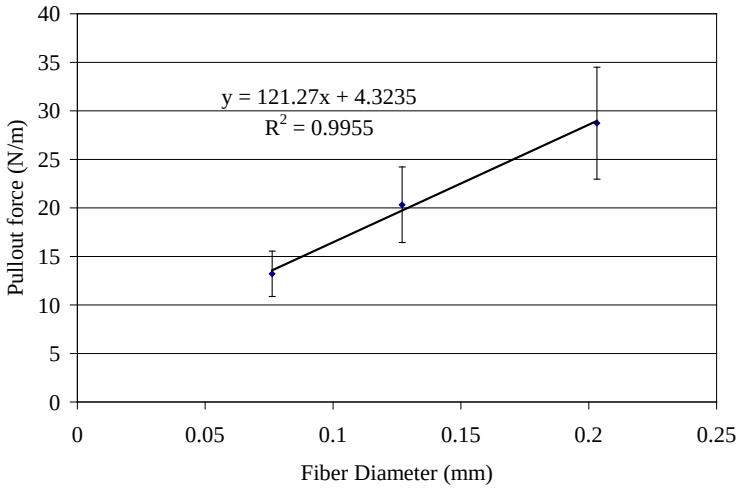

Figure 2. Pullout Force for FEP Monofilaments in Epon 862/W Cured Resin.

The disadvantage of this vascular network technique is that it is not autoclave compatible. In the presence of carbon fibers, these FEP fibers are embossed by the carbon fibers, which hinders the pullout extraction. This technique is suited for VARTM layups.

Embedded Tubes

Embedded tubes can span a large range of possible diameters. We examined 304 stainless steel tubes for this work. The smallest size that we worked with is 203 µm outside diameter and 102 µm inside diameter. These tubes are well suited for all processing techniques, including autoclave. When incorporated within unidirectional carbon fiber prepreg, it is best to run these tubes parallel to the fiber tows, where they readily submerge into those tows. Running them perpendicular to the tows causes substantial fiber displacement that is readily visible in two-ply layups.

Embedded tubes are useful for manufacturing isolated vascular networks, which could be used for cooling fluids or high pressure networks. The difficulty with these networks arises with branching and macroscopic connection techniques, which as discussed in the next section.

Manifolds

A critical consideration for any vascular network fabrication technique is the connection to a macroscopic fluid system. The connection choice is greatly influenced by the pressures involved with pumping the fluid through the network. In general, the pressure does follow the Hagen- Poiseuille relation ship in Eq. 1. Figure 3 shows flow rate vs. pressure data for 25°C water flowing through an unlined 203µm passage manufactured with an extractable fiber technique. It is apparent that the pressures can quickly reach 15 atm and beyond.

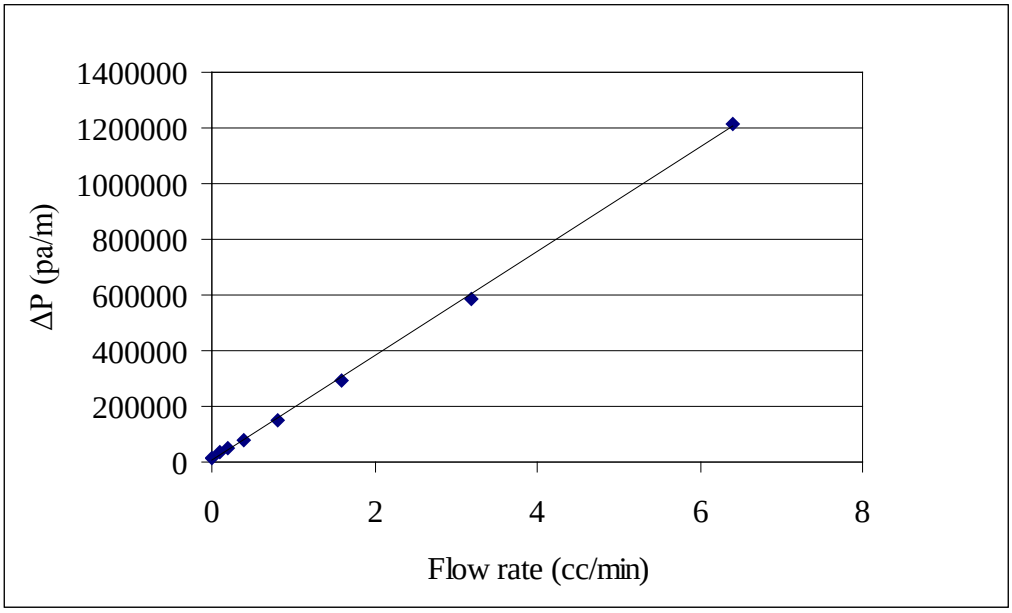

Figure 3. Pressure drop vs. flow rate for a 203µm, unlined passage with water at 25°C. The blue markers are experimental data and the line is from the Hagen-Poiseuille relation.

Three main solutions have been developed for this issue, though many other possibilities exist. The first is to cast an entry tube into the composite and have the vascular passages branch from there where they are sealed to the entry tube by the composite resin. This works well for unlined passages. The second is to bundle the tubes from lined passages and either glue or solder them into a manifold. The third is to machine a hole in the composite where either lined or unlined passages converge and use a Banjo bolt type connection to make the fluid connection.

Thermal

Some of the potential of incorporating microvascular networks into composites was demonstrated for thermal aspects. Figure 4 shows the thermal image for a composite panel with a microvascular passage sitting on a hot plate. The potential of this technique to utilize the skin composites of aircraft for multifunctional capabilities is quite realistic. Other capabilities, such as damage detection and self-healing, still warrant investigation.

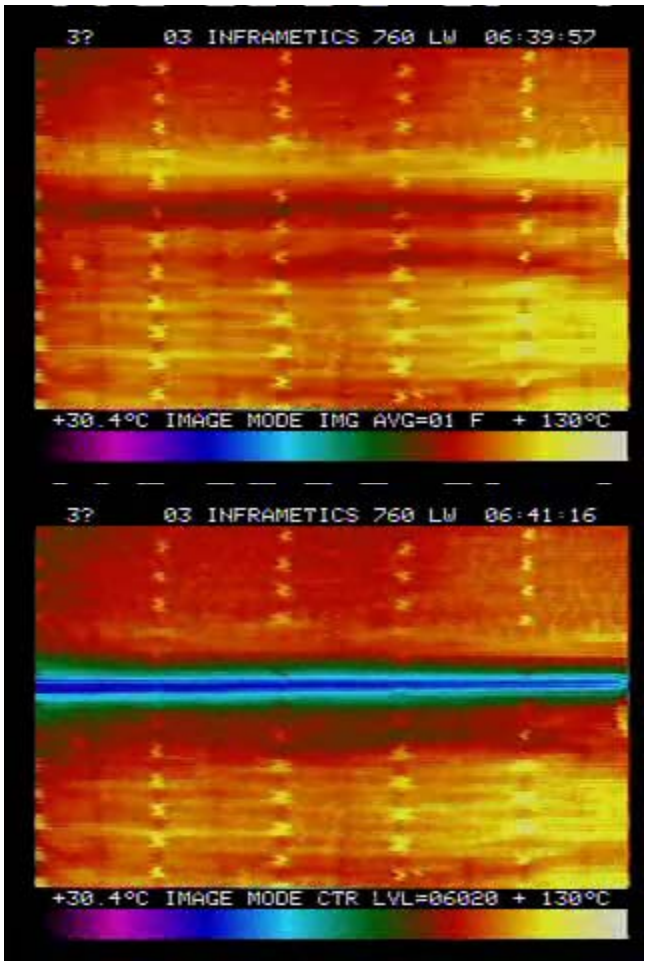

Figure 4. A 508µm thick panel of IM7 with Epon862/W. A single 102µm ID and 203µm OD 304 stainless steel lined passage is in the middle. The panel is on a 110°C hotplate. The thermal image should the difference between no flow (top) and 2ml/min water entering at 25°C (bottom). The cooled width is ~30 times the capillary diameter.

Granular

Some of the vascular work has focused on the inverted vascular network, where a fluid surrounds micron sized particles. These materials are referred to as granular solids. Depending on the applied granular bed pressure, these materials demonstrate a yield behavior, leading to liquid-like and solid-like states. We investigated the potential of these materials to be used for morphing and variable stiffness applications. This work is represented in the journal article by Phillips, *et al.* (SAMPE Fall Technical Conference Proceedings, 2007), where the flexural properties of granular reinforced bending sections were examined. The file is attached.

Presentations

D.M. Phillips, G.S. Jacobson, and J. Baur, "Granular Reinforced Materials for Morphing Structures," 2007 SAMPE Fall Technical Conference and Exhibition, Cincinnati, OH, Oct. 29-Nov. 1, 2007.

D.M. Phillips, F.J. Khan, M.D. Negilski, G.S. Jacobson, and J.W. Baur, "Novel Activation and Deformation Mechanics of Reinforced Shape Memory Polymer Composites for Morphing Aerostructures," 2006 MRS Fall Meeting, Presentation A1.5, Dynamic Modulus, Shape Memory and Gels, Boston, MA, Nov. 27-Dec. 1, 2006.

Publications

D.M. Phillips, F.J. Khan, G.S. Jacobson, and J.W. Baur. "Granular Reinforced Materials for Morphing Structures," SAMPE Fall Technical Conference Proceedings CD ROM, 7 pp. (2007).

References

---

[i] R. Vaia, J. Baur, *Science* 319(5862), pp. 420-421 (2008).

APPENDIX:

GRANULAR REINFORCED MATERIALS FOR MORPHING STRUCTURES

David M. Phillips†, Fazeel J. Khan‡, Gabriel S. Jacobson†, and Jeffrey W. Baur†
† *Materials and Manufacturing Directorate, WPAFB, OH 45433*
‡ *Miami University, Oxford, OH 45056*

ABSTRACT

The variable flexural stiffness and strength of granular reinforced composite sections were investigated as a function of applied confinement pressure. The impact of particle size and shape on the resulting mechanical properties was examined using different sizes of hollow glass bubbles and dodecahedral almandite powder. The result is a reversible, self-healing locking mechanism that exhibits a fifty-fold increase in flexural modulus and a ten-fold increase in flexural strength with the simple application of vacuum to confine the granular media. In comparison to thermally triggered shape memory polymers, this approach has the potential to avoid the complications caused by low thermal conductivity and triggering complications due low and high temperature environments. Since the granular media can be readily transported between chambers, structures that adaptively reinforce themselves in response to changing loads can be envisioned.

KEY WORDS: Smart Materials/Smart Structures, Microspheres/Microballoons, Hybrid Materials/Structures

1. INTRODUCTION

Materials for morphing aerostructures face the conflicting requirements of needing a low modulus combined with the capability of large deformations while undergoing a shape change and being both stiff and strong while in the desired locked configuration. One approach to span this modulus requirement is the use of shape memory polymers (SMPs). These materials are typically lightly cross-linked polymers that have been optimized to have good elastic properties in the rubbery regime above the glass transition temperature (T_g), the capability of changing its modulus by several orders of magnitude, and the ability to store strain energy in the glassy state. For example, if a material is deformed in the rubbery state and then fixed by cooling through the T_g to the glassy state, the strain energy of that configuration is stored in the material. When the same material is then heated above T_g while unconstrained, the material attempts to return to or "remember" the original shape by releasing that strain energy. SMPs have some problems since most are thermally activated, which causes the activation of devices to be kinetically limited by the low thermal conductivity of the polymer resin. Heating beyond T_g may also require excessive energy when activated in cold environments. Conversely, SMPs may also be activated by uncontrolled thermal sources in the environment if the temperature exceeds T_g. An alternative approach to achieving the variable stiffness of SMPs is vacuum activated granular media confinement, which offers a modulus tuning methodology that is faster, requires less energy, and is less influenced by the operating environment.

Granular media have the ability to exhibit liquid-like and solid-like states depending on their interparticle spacing. Below the random close packing (RCP) threshold, there is essentially zero confinement pressure acting on the media and a free-flowing, liquid-like state exists. Once the RCP threshold is met, the granular media percolates and forms force chains due to particle jamming, resulting in a phase change to a solid-like state (1, 2). The reported RCP threshold volume fraction for monodisperse spheres varies between 0.60 and 0.68 (2-4). Torquato *et al.* further define the RCP threshold state for monodisperse spheres as a jammed state with the maximum randomness to arrive at a volume fraction of 0.64. Faceted or irregular media are expected to exhibit a jammed state at a lower volume fraction than spheres.

Above the RCP threshold, the bulk modulus (K) and the shear modulus (μ) of the granular media vary as a function of confinement pressure (p) (3-7). The bulk modulus of granular media is typically measured experimentally by monitoring the acoustic response at a wavelength that is longer than the size of the granular particles. (3-5). The effective medium theory predicts that the moduli will scale as $p^{1/3}$ (3,6,7), however, reported experimental data tends to scale as $p^{1/2}$ (3,5,7). Both scenarios lead to a situation where the modulus of the granular media can be tuned as a function of confinement pressure. For example, experimental values for glass beads (45 μm diameter) can vary from 300 MPa to 5 GPa for the bulk modulus K and 40 MPa to 3 GPa for the shear modulus μ with the application of 1 to 100 MPa of confinement pressure (3). In this paper, the modulus variation across the RCP threshold is investigated with the application of a confinement pressure of only 0.1 MPa (atmospheric pressure). It is interesting to note that greater enhancements in modulus can be achieved beyond those demonstrated here by simply increasing the confinement pressure.

The phase change and tunable moduli of granular media make them attractive as reinforcement for dynamic modulus composite devices. Since the granular media can withstand compression and shear loading better than tensile stress, composites must be designed such that tensile loads are carried by the container while also allowing the granular confinement pressure to be modulated. In this work, one such composite device is designed, fabricated, and analyzed for variation of flexural modulus and strength using hollow glass bubbles or almandite garnet [base formula $Fe_3Al_2(SiO_4)_3$] as the granular media.

2. EXPERIMENTAL

2.1 Granular Media Four types of granular media were examined in this work. Two are low density glass microbubbles (Scotchlite Glass Bubbles, 3M, St. Paul, MN) and two are almandite garnet waterjet abrasives (Barton Mines Company, LLC, Lake George, NY). The properties of the granular media are listed in Table 1.

TABLE 1: PROPERTIES OF GRANULAR MEDIA

Granular Media	Median Diameter (μm)	Particle Density (g/cc)	Packed Density (g/cc)	Surface Treatment
Scotchlite A20 Glass Bubbles	60	0.20 [a]	0.13 [b]	methacrylato chromic chloride [a]
Scotchlite D32 Glass Bubbles	40	0.32 [a]	0.20 [b]	methacrylato chromic chloride [a]
Almandite 120 grit	125	3.9-4.1 [c]	2.07 [d]	n/a
Almandite 220 grit	75	3.9-4.1 [c]	1.99 [d]	n/a

a: information from product brochure
b: particle density multiplied by a 0.64 volume fraction for RCP
c: value from product MSDS
d: density measured for 250cc of packed media

The Scotchlite glass bubbles are soda-lime-borosilicate glass microspheres. The bulk density of soda-lime-borosilicate glass is 2.23g/cc, which indicates that the Scotchlite bubbles are mostly hollow. The bubbles are free-flowing when not confined and can be easily pumped through a silicone rubber hose of 0.125 in inside diameter with a syringe.

The almandite abrasives were chosen due to the faceted nature of the media. Almandite exhibits a dodecahedral crystal habit, which could lead to a higher volume fraction than hexagonally close packed spheres, where $\phi_{HCP} = 0.74$. In practice, the facets on the crystals caused the onset of jamming to occur at a lower volume fraction measured between 0.49 and 0.53. Although the almandite was more difficult than the Scotchlite bubbles to pump through a tube, it remained free-flowing with the consistency of dry sand.

2.2 Test Sections The flexural test sections used for this work were manufactured from 0.020 in thick G10/FR4 sheets (Accurate Plastics Inc., Yonkers, NY) and 0.03125 in thick, 50A durometer silicone rubber sheets (McMaster-Carr, Atlanta, GA). The G10/FR4 sheets were cut into 1.5 in x 12 in pieces to make the top and bottom of the test section. These pieces were separated by 1 in and bonded along the inside seams to 1.040" x 12" pieces of the silicone rubber sheet using RTV silicone adhesive to make the specimen displayed in Fig. 1. The ends of the test sections were capped with 0.125 in thick, 50A durometer silicone rubber pieces bonded with RTV silicone adhesive. The end caps were drilled and bonded to silicone rubber tubes (0.25 in outside diameter and 0.125 in inside diameter) to permit filling on one end and application of vacuum on the other. The vacuum application side was plugged with cotton to prevent the granular media from escaping the test sections. Each test section was leak tested under water by applying a small positive pressure prior to being filled with granular media.

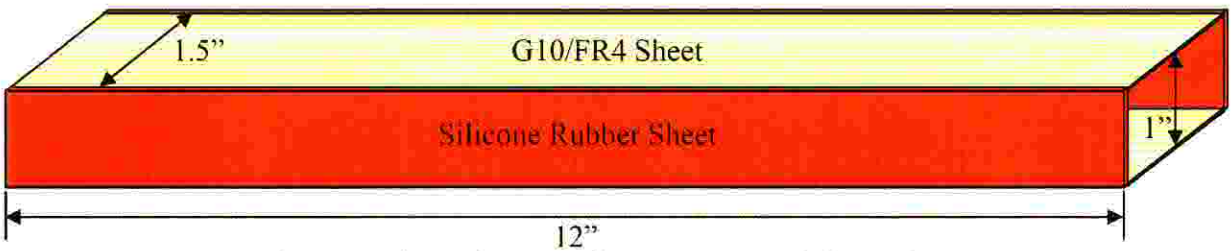

Figure 1. Flexural test section structure and dimensions.

Two of the test sections were modified by the addition of solid reinforcement pieces. The first was simply an addition sheet of a 1 in x 0.020 in thick G10/FR4 at the neutral axis of the test section. The second internal reinforcement section investigated was a 1 in x 0.5 in piece of honeycomb core with a 0.25 in hexagonal spacing perpendicular to the neutral axis. Neither reinforcement piece significantly affected the stiffness of the unfilled test sections.

The test sections were filled with granular media using syringe injection for the glass bubbles and a gravity feed for the almandite. Each test section was tapped while being filled until approximately 95% of the section volume capacity was occupied. This small void space allowed the granular media to exhibit a liquid-like state. After filling, the fill port was plugged and clamped.

The modulus transitions of the composite specimens were activated by applying a rough vacuum (<7 kPa) to the vacuum ports. Much of the confinement pressure was supplied by the section volume contraction that was allowed by the flexible silicone rubber sides. Assuming mechanical equilibrium, the confinement pressure on the trapped granular media is equal to the pressure difference between the atmosphere and applied vacuum (~0.1 MPa). The sections became firm within 15 seconds and reached full stiffness within several minutes as the residual air percolated through the jammed granular media. The test sections were sufficiently robust to endure mechanical deformation in the activated or deactivated states without causing damage. Once activated and sealed, the composites maintain their shape until mechanically perturbed or the vacuum is released. These filled sections were also reusable for multiple mechanical tests.

2.3 Three-Point Bending Tests and Calculations The three point bending tests followed Procedure B of ASTM Standard D 790-03 with the exception of the span (8). The ASTM standard recommends a 16:1 minimum span to thickness ratio. However, we used only a 10 in span due to the limitations of our three-point testing fixture, which results in an approximate 10:1 span to thickness ratio. An MTS model 312.2 test frame equipped with an MTS model 661.21A-01 load cell was used for all mechanical measurements. Loading of the sections was performed at 0.10 in/in/min to a total flexural strain (ε_f) of 5% , where ε_f is calculated using

$$\varepsilon_f = 6Dd/L^2, \qquad [1]$$

Here, D is the deflection at the center of the section, d is the section thickness, and L is the span of the section. The value for L is fixed at 10 in. The value for d was measured for each section before starting the loading.

The flexural stress was calculated as

$$\sigma_f = 3PL/2bd^2, \qquad [2]$$

where P is the applied load and b is the width of the section. The value for b is fixed at 1.5 in.

The loading curves for all of the sections have a linear, elastic regime for small strains followed by a plastic deformation regime in which the granular media redistributes within the section.

None of the samples permanently yielded or broke and could be restored to their original shape by releasing and reapplying vacuum. The modulus of elasticity in bending, E_B, and the strength at ε_f=0.05, $\sigma_{f\_0.05}$ was reported for each samples. The modulus of elasticity is calculated as

$$E_B = L^3m/4bd^3, \quad [3]$$

where m is the initial straight line slope of the load (P) as a function of displacement (D). The value for $\sigma_{f\_0.05}$ is determined from Eq. 2, where the linear plastic deformation portion of the stress-strain plot is fit with a line and $\sigma_{f\_0.05,}$ is calculated at ε_f=0.05.

3. Results

3.1 Three Point Bending Test Results A total of six test sections were tested five times each in both the deactivated and activated (vacuum applied) states. Table 2 lists the test sections and their designation.

TABLE 2: TEST SECTIONS

Section	Granular Media	Section Reinforcement
120_grit	Almandite 120 grit	n/a
220_grit	Almandite 220 grit	n/a
D32	Scotchlite D32 Glass Bubbles	n/a
A20	Scotchlite A20 Glass Bubbles	n/a
A20_mid	Scotchlite A20 Glass Bubbles	Neutral axis 0.020 in G10/FR4 sheet 1 in wide
A20_hex	Scotchlite A20 Glass Bubbles	Neutral axis hexagonal paper grid, 1 in wide, 0.5 in thick, 0.25 in hexagonal spacing

The resultant mechanical data are displayed in Fig. 2. The 120_grit and 220_grit sections with almandite media had a significantly higher deactivated bending modulus (E_B) and strength ($\sigma_{f\_0.05}$) compared to the A20 and D32 glass bubble sections. This is likely due to the lower jamming threshold of the faceted almandite media. The activated E_B for the almandite media was not significantly larger than the unreinforced glass bubbles within the 95% confidence interval, however, the $\sigma_{f\_0.05}$ is significantly higher.

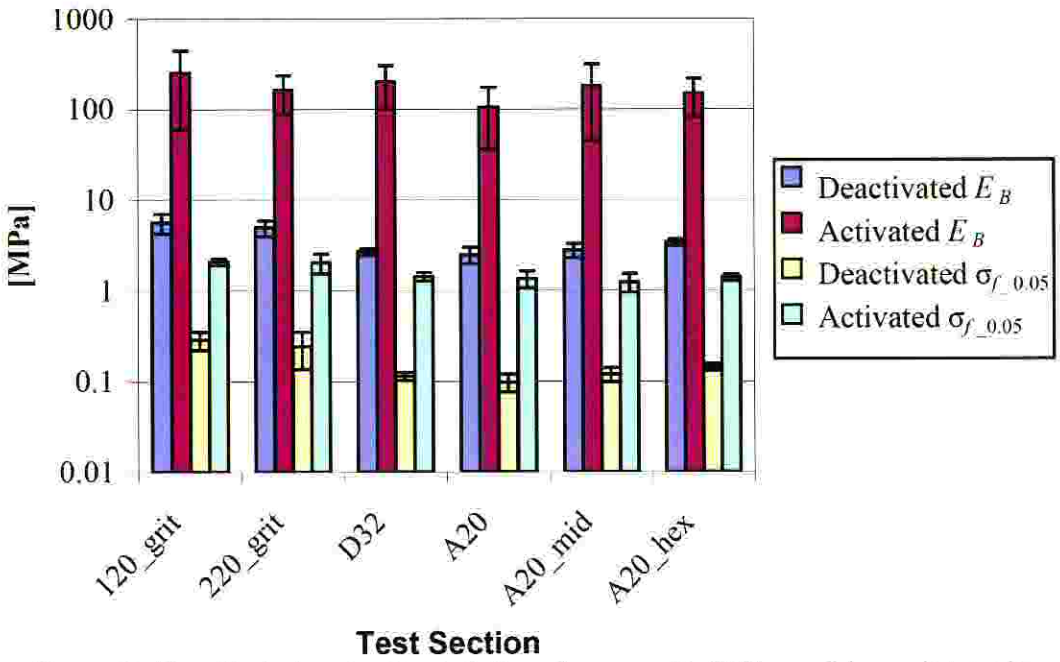

Figure 2. Deactivated and activated E_B and $\sigma_{f\_0.05}$ with 95% confidence intervals.

The A20 glass bubble media was selected for investigation in the neutral axis reinforced sections. The intent of the reinforcement was to increase the shear in the confined granular media and provide anchor points for the force chains. The deactivated E_B and $\sigma_{f\_0.05}$ for the A20_hex section was significantly larger than the A20 section. The deactivated A20_mid section had a significantly larger $\sigma_{f\_0.05}$ than the A20 section. Since the only significant difference in the properties occurs in the deactivated states, the difference is most likely attributable to the mechanical enhancement of adding the neutral axis reinforcement. The mechanical enhancement becomes insignificant in the activated state.

The ratio between the activated and deactivated values of E_B and $\sigma_{f\_0.05}$ is a relative measure of the dynamic range of the modulation and is of interest for a variety of applications, including shape changing structures, vibration damping, and controlled mechanical coupling. Since the measured values have contributions from the silicone and fiber test section, an inherently stiffer section will yield a lower dynamic ratio. With the exception of the neutral axis reinforced sections, the other sections in these tests are equivalent. Table 3 lists the dynamic ratios and confidence intervals for all of the filled test sections as a function of particle type and neutral axis reinforcement.

TABLE 3: DYNAMIC RATIOS FOR TEST SECTIONS

Section	120_grit	220_grit	D32	A20	A20_mid	A20_hex
$E_{B,\ activated}/E_{B,\ deactivated}$	44.77	32.85	74.96	42.17	64.24	44.19
Upper 95% CI	105.35	59.93	123.62	88.09	136.70	70.20
Lower 95% CI	8.35	14.90	33.92	12.05	13.60	22.25
$\sigma_{f\_0.05,\ activated}/\sigma_{f\_0.05,\ deactivated}$	7.23	8.37	12.54	13.89	10.42	9.72
Upper 95% CI	10.13	18.61	15.56	21.61	15.54	11.57
Lower 95% CI	5.39	4.38	10.08	8.97	6.83	8.16

From the ratio data, it is evident that the vacuum activation mechanism allows for tuning of both E_B and $\sigma_{f\_0.05}$. This property change includes both a phase transition and compaction within the granular solid media with the application of a confinement pressure. As discussed earlier, the confinement pressure applied within this study was approximately 10% to 0.01% of the pressure applied by other researchers to achieve bulk modulus values on the order of several GPa. It is anticipated that significantly higher dynamic ratio could be achieve using composite designs with either a larger range of confinement pressure and/or a variable stiffness matrix (SMP, etc.) that can be made to be more compliant than the current design.

4. CONCLUSIONS

Compaction of confined granular media is a viable mechanism for varying both the modulus and strength of a filled composite device. Future work warrants combining granular reinforcement with other novel designs to potentially yield a variable stiffness composite with an even larger dynamic range. Such design philosophy could be used for low activation energy morphing aerostructures.

4. REFERENCES

1. S. Ostojic, E. Somfai, and B. Nienhuis, Nature, **439**, 828 (2006).
2. S. Torquato, T.M.Truskett, and P.G. Debenedetti, Phys. Rev. Lett., **84**(10), 2064 (2000).
3. H.A. Makse, N. Gland, D.L. Johnson, and L.M. Schwartz, Phys. Rev. Lett., **83**(24), 5070 (1999).
4. X. Jia, C. Caroli, and B. Velicky, Phys. Rev. Lett., **82**(9), 1863 (1999).
5. J.D. Goddard, Proc. R. Soc. Lond. A, **430**(1878), 105 (1990).
6. K. Walton, J. Mech. Phys. Solids, **35**(2), 213 (1987).
7. P.-G. de Gennes, Europhys. Lett., **35**(2), 145 (1996).
8. ASTM Standard D 790-03, Flexural Properties of Unreinforced and Reinforced Plastics and Electrical Insulating Materials, American Society for Testing and Materials, West Conshohocken, Pennsylvania, 2003, pp.1-11.